FLUID MECHANICS OF MUSCLE VIBRATIONS

DANIEL T. BARRY AND NEIL M. COLE
Department of Physical Medicine and Rehabilitation and Bioengineering Program, University of Michigan Medical Center, 1500 E. Medical Center Drive, Ann Arbor, Michigan 48109-0042

ABSTRACT The pressure field produced by an isometrically contracting frog gastrocnemius muscle is described by the fluid mechanics equations for a vibrating sphere. The equations predict a pressure amplitude that is proportional to the lateral acceleration of the muscle, inversely proportional to the square of the distance from the muscle, and cosinusoidally related to the major axis of lateral movement. The predictions are confirmed by experiments that measure the pressure amplitude distribution and by photographs of muscle movement during contraction. The lateral movement of muscle has the appearance of an oscillating system response to a step function input—the oscillation may be at the resonant frequency of the muscle and therefore may provide a means to measure muscle stiffness without actually touching the muscle.

INTRODUCTION

Pressure waves are produced by contracting skeletal muscle. The root mean-squared (RMS) pressure increases with increasing force of contraction; with strong, sustained, voluntary contraction, sounds are audible at the skin surface and have a low frequency, rumbling quality. (Oster and Jaffe, 1980; Barry et al., 1985) A stimulated muscle twitch produces a burst of pressure change that has a characteristic waveform of oscillations that initially increase in amplitude and then decrease. The waveform from a particular muscle varies with the length of the muscle, peak twitch force, and temperature—if these are constant then the pressure signal demonstrates essentially no variation from one twitch to the next. Previous work has demonstrated that the pressure waves are related to lateral movements of muscle (Barry, 1987; Frangioni, et al., 1987). Here we develop a quantitative description of muscle pressure wave production in vitro and report that the pressure field is described by a dipole model with the pressure amplitude directly related to, and in phase with, the lateral acceleration of the muscle.

METHODS

Frog (rana pipiens) gastrocnemius muscles were isolated and removed with the nerve supply intact from cold-anesthetized animals. The tendons were sutured to small steel hooks with monofilament suture. The muscles were suspended between a force transducer (model F5A-1; Konigsberg Instruments, Pasadena, CA) and a micrometer and placed in a bath of frog ringers (115 mM NaCl, 2.5 mM KCl, 1.8 mM $CaCl_2$, 2.15 mM Na_2HPO_4, 0.85 mM NaH_2PO_4) (Julian and Morgan, 1979). The apparatus was constructed to allow both rotation of a hydrophone around the long axis of the muscle and variation in the muscle to hydrophone separation (Fig. 1). For the isometric contraction experiments, muscle force and length were monitored with a servomotor (model 305; Cambridge Technology, Inc., Watertown, MA) in place of the fixed post. The concentric contraction experiments were performed with two different protocols. In one, the muscle was suspended on hooks between a light spring (spring mass = 0.06 g, spring constant = 3.0 g/cm, Grass Instrument Co.) and either a fixed post or a force transducer. In the second protocol, the muscle was suspended between a servomotor and a fixed post. The servomotor was set to provide minimal resistance to contraction while monitoring the linear movement of the end of the muscle. Accelerations were calculated digitally by differentiating the position signal twice over time.

In some experiments two hydrophones (model 8103; Bruel and Kjaer Instruments, Inc., Marlboro, MA) were used to either record acoustic signals from two different points in the bath simultaneously or to provide an active hydrophone and a distant reference hydrophone for differential recordings. The two hydrophones used were individually calibrated by Bruel and Kjaer Instruments, Inc. and found to have a frequency response that was flat to ±1 dB over a range of 1.0 Hz to 30 KHz and flat to ±3 dB over 0.1 Hz to 150 KHz. The hydrophone signal was amplified with a charge amplifier (model 2635; Bruel and Kjaer Instruments, Inc.); filter settings were set at 2 Hz low frequency cutoff and 1.0 KHz high frequency cutoff. The muscle was stimulated with a stimulator (model S88; Grass Instrument Co., Quincy, MA) and a stimulus isolation unit (model SIU-5; Grass Instrument Co.) via a suction electrode attached to the stump of the severed sciatic nerve. Stimulation voltage was increased slightly above the level at which maximal twitches were obtained. Optimal length (L_0) was defined as the length at which the largest force was obtained. Data were recorded digitally using 12 bit analog-to-digital conversion with 0.4 ms sampling of force and acoustic signals.

Photographic records of muscle movement were obtained with high-speed cinematography and with 35 mm frames exposed with a timed strobe light. Cinematography was performed with a 16 mm high-speed motion picture camera (model DBM-45; Redlake Corp. Inc., Morgan Hill, CA) set for 500 frames/second speed to obtain 2.0 ms sampling of muscle movement during contraction. A 35 mm camera (model x-370; Minolta Camera Co. Ltd., Osaka, Japan) with a macro lens was used with a strobe light (model 136, Chadwick-Helmuth Co., Inc., Monrovie, CA) to obtain a series of "stop-action" exposures of much higher quality than individual frames of the cine film. The strobe was triggered once for each photograph. The trigger was delayed from the time of the stimulus by successive 5 ms intervals up to 100 ms to obtain 20 exposures from 20 stimulations. The separation of the hydrophone and the muscle was measured from an identifiable point on the muscle belly along a line perpendicular to the long axis of the muscle.

Please address all reprint requests to Dr. Barry.

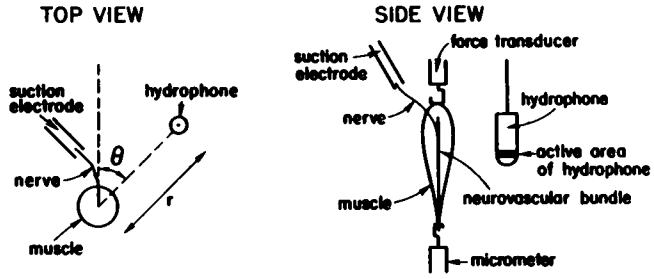

FIGURE 1 A diagram of the geometry used in the experiments shows r and θ. θ = 0° was defined as the orientation that corresponds to the neurovascular bundle that runs longitudinally along the gastrocnemius muscle. The major plane of muscle movement was determined by adjusting the hydrophone's vertical position to obtain the maximal response; the maximum was always near the mid-point of the muscle.

RESULTS

Fig. 2 *a* shows an example of a typical pressure signal. This signal shows the characteristic pattern of oscillations that rise in amplitude and then decay (Barry, 1987; Frangioni et al., 1987). If the hydrophone is rotated about the long axis of the muscle, there are usually two azimuths 180° apart that record a signal of maximal amplitude in the first half-cycle. These aximuths and the long axis of the muscle define a plane that contains the earliest and the dominant mode of lateral oscillation. The amplitude of pressure does not vanish with the hydrophone placed orthogonal to the dominant mode, indicating that other modes are present. The summation of all modes produces the characteristic rising and then decaying oscillations seen with an arbitrary placement of a hydrophone.

Using fluid mechanics equations, we can predict the pressure field produced by an arbitrary function of muscle movement. The fundamental equation describing the propagation of small amplitude acoustic signals in an adiabatic and inviscid fluid is (Ziomek, 1985)

$$\nabla^2\phi(t, \mathbf{r}) - \frac{1}{c^2(\mathbf{r})}\frac{\partial^2\phi(t, \mathbf{r})}{\partial t^2} = Z(t, \mathbf{r}) \tag{1}$$

where $\phi(t, \mathbf{r})$ = velocity potential at time t, position $\mathbf{r}$ $Z(t, \mathbf{r})$ = source distribution $c(\mathbf{r})$ = speed of sound in the medium also, $u(t, \mathbf{r}) = -\nabla\phi(t, \mathbf{r})$ where $u(t, \mathbf{r})$ = acoustic fluid (particle) velocity.

For constant, c, Eq. 1 has a general solution

$$\phi(t, \mathbf{r}) = \frac{1}{4\pi}\int_{V_o}\frac{Z(t - |\mathbf{r} - \mathbf{r}_o|/c, \mathbf{r}_o)}{|\mathbf{r} - \mathbf{r}_o|}\,dV$$

where $\mathbf{r}_o$ = location of an element of the source and V_o is the volume that the source occupies.

If we assume that the density, ρ_o, of the medium is constant then the pressure field $p(t, \mathbf{r})$ is obtained by the relationship

$$p(t, \mathbf{r}) = \rho_o\frac{\partial\phi(t, \mathbf{r})}{\partial t} \tag{2}$$

Analytical solutions to Eq. 2 are difficult to obtain unless simplifying assumptions are made. If we roughly model the muscle as a harmonically vibrating sphere, then Eq. 2 can be expanded to obtain an explicit relationship between pressure and surface velocity. (Ross, Eqs. 9.6, and 9.10, 1987).

$$p_{res}(t, r, \theta) = \frac{-w\rho_o S_o u_o}{4\pi r}\left(\frac{ka_o}{2}\cos\theta\right)e^{i(wt-kr)} \tag{3a}$$

$$p_{react}(t, r, \theta) = \frac{iw\rho_o S_o u_o}{4\pi r^2}\left(\frac{a_o}{2}\cos\theta\right)e^{i(wt-kr)} \tag{3b}$$

$$p_{total}(t, r, \theta) = p_{res}(t, r, \theta) + p_{react}(t, r, \theta) \tag{3c}$$

where $p_{total}(t, r, \theta)$ = total pressure amplitude in Pascals.

$p_{res}(t, r, \theta)$ = pressure corresponding to radiation resistance, representing the far-field pressure of dipole radiation (Pascals). $p_{react}(t, r, \theta)$ = pressure corresponding to the reactive component of the dipole radiation, representing near-field hydrodynamic sloshing (Pascals). w = angular frequency of oscillation in radians/second. u_o = maximum velocity in meters/second. Instantaneous velocity is $u = u_o e^{iwt}$ and instantaneous acceleration = iwu. The magnitude of maximal acceleration is wu_o. ρ_o = constant equilibrium density of the medium in kilogram/(meter)^3. a_o = radius of the sphere in meters. S_o = area of the sphere = $4\pi a_o^2$ in meters^2. r = distance from source to hydrophone in meters. k = wave number = $2\pi/\lambda = w/c$ in meters^{-1}. c = speed of sound in the medium in meters/second.

θ = azimuth of hydrophone from the axis of vibration (radians), and we assume that the wavelength of the acoustic signal is much larger than the radius of the source. The assumption that the source is small compared with wavelength ($ka \ll 1$) is valid in our case since (ka) is $\sim 10^{-4}$.

Eq. 3 *a* describes the pressure corresponding to the radiation resistance, the dominant factor in the far-field, when kr $\gg$ 1. In our case, kr is $\sim 10^{-4}$ and the reactance term (Eq. 3 *b*) dominates the result. Under these near-field conditions, pressure is directly proportional to the surface acceleration (iwu). This result implies that the pressure is proportional to the acceleration of the muscle surface or, alternatively, that the second integral over time of pressure is proportional to the position of the muscle surface. Eq. 3 *b* indicates that, under near-field conditions, the pressure decays as the square of the distance from the source. If we improve the muscle model by replacing the vibrating sphere with a vibrating cylinder of long, thin dimensions, then the pressure should decay inversely with distance near the cylinder. The Appendix demonstrates a specific calculation of muscle pressure wave amplitude.

The total pressure field is described by the vector sum of the near-field and far-field pressures. The near-field wave that dominates the pressure field in these experiments is a form of hydrodynamic sloshing rather than a propagated sound wave. The propagated sound wave corresponds to

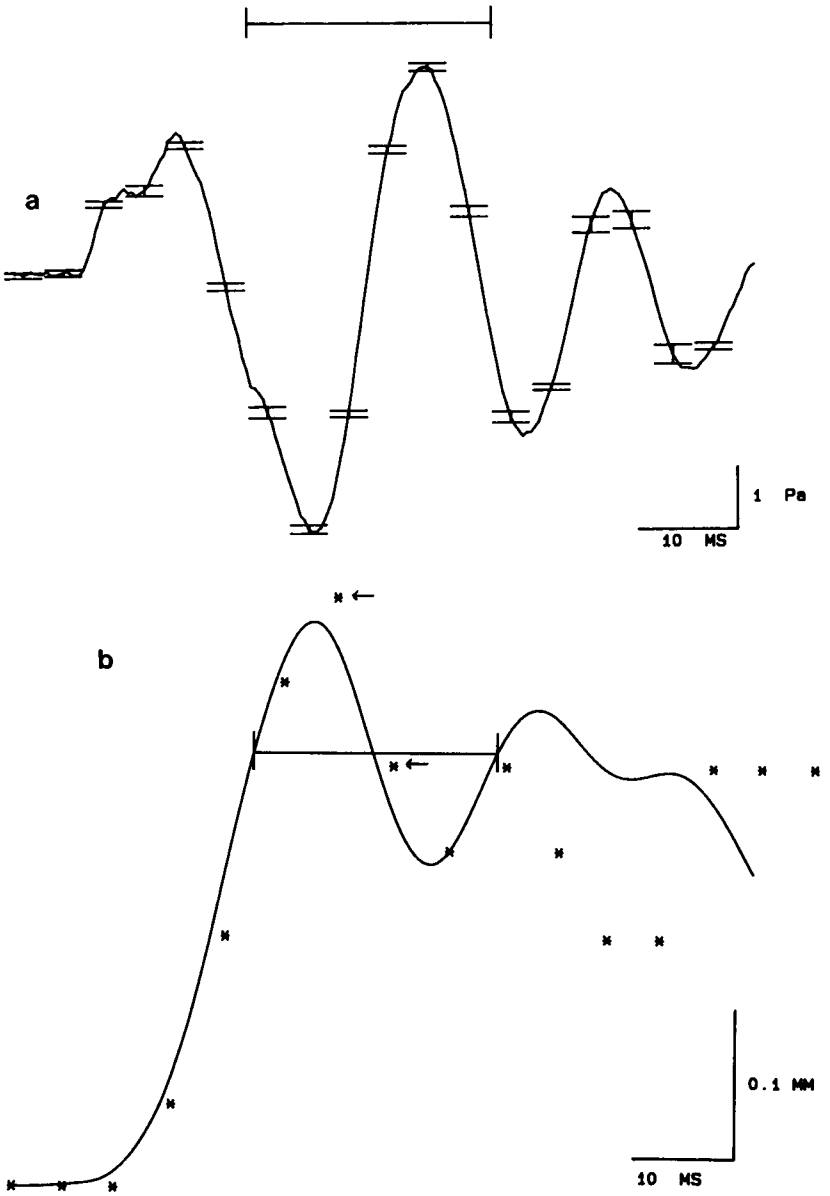

FIGURE 2 (*a*) The acoustic signal obtained at a distance of r = 1.2 cm and an azimuth of 0° shows rising and decaying oscillations. The figure shows the averaged response from eight stimulations; error bars denote standard deviations and are shown for every twelfth point. The bar shows the time of calculation of pressure amplitude for comparison to the amplitude predicted by Eq. 3 b in the text. The peak-to-peak amplitude is 7.6 Pa so the value corresponding to pressure amplitude in Eq. 3 b is 3.8 Pa. (*b*) The second integral over time of the waveform in *a* demonstrates a large low frequency component with superimposed high frequency components. The distances between the muscle and the hydrophone as measured from photographs during a twitch (*) are close to the distances predicted using the double integral of the acoustic signal (*solid line*) for ~60–70 ms. The bar shows a segment of data that roughly approximates one cycle of harmonic vibration. The arrows indicate data points used in approximating the lateral velocity of muscle movement.

the far-field solution, declining inversely with distance from a vibrating sphere and 90° out of phase with the near-field solution. Muscles are inherently poor low frequency sound generators because the size of the muscle is very small compared with the wavelength of the sound.

To check the predictions of the equations we monitored the position of the muscle with respect to the hydrophone using high speed cinematography and 35 mm slides exposed with a strobe light. Differentiating the muscle position function twice to obtain muscle acceleration produced a noisy function due to the small number of points in the function. We used the alternative procedure of integrating the pressure signal twice over time to obtain a function that Eq. 3 *b* predicts should be proportional to muscle position. Fig. 2 shows that lateral muscle position and the second integral over time of sound were similar functions, for ~60–70 ms after stimulation. Beyond ~70 ms the integral becomes inaccurate due to cumulative effects of small DC shifts and low-frequency noise. The absolute amplitude of pressure predicted by Eq. 3 *b* can be compared with the experimental value by using the section of data marked by the bar in Fig. 2 as representative of harmonic motion. The Appendix contains detailed calculations of the predicted pressure amplitude (half the peak-to-peak value) of 3.5 Pascals (Pa) which compares well with the experimental value of 3.8 Pa.

Pressures recorded near the long axis of a concentrically contracting muscle were directly related to the linear acceleration of the muscle. Fig. 3 *a* shows the force record produced by a concentrically contracting muscle with a spring placed between the muscle and the force transducer. Fig. 3 *b* shows the data obtained when the spring is between the muscle and the micrometer. In this configuration, the force transducer recorded a spike corresponding to

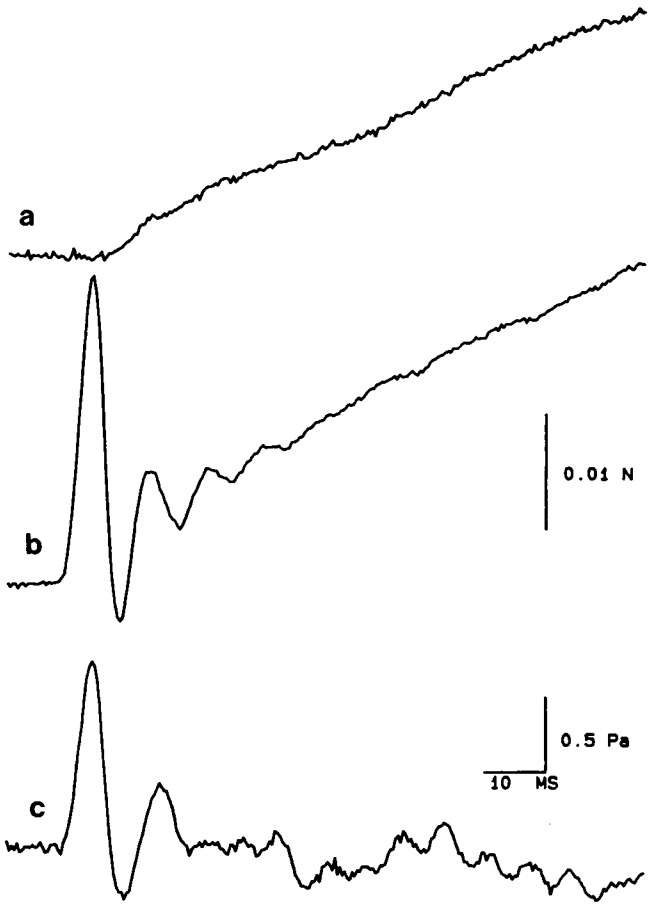

FIGURE 3 (*a*) The force record obtained during a tetanic concentric contraction with the spring between the muscle and the force transducer shows a smoothly increasing force. The waveform is the averaged response from four stimulations. Temperature for all three records (*a*, *b*, *c*) was 15.7 ± 0.5°C. (*b*) Placing the spring between the fixed post and the muscle allows the force transducer to record the force due to acceleration of muscle mass as well as the force stretching the spring. The waveform is the averaged response from eight stimulations. (*c*) A tetanic concentric contraction produced pressure signals near the long axis of the muscle that correspond to linear accelerations of the muscle. See the appendix for specific calculations of the relationship between acceleration and pressure amplitudes. The hydrophone was placed near the tendon at the end of the muscle opposite the spring. The waveform is the averaged response from four stimulations.

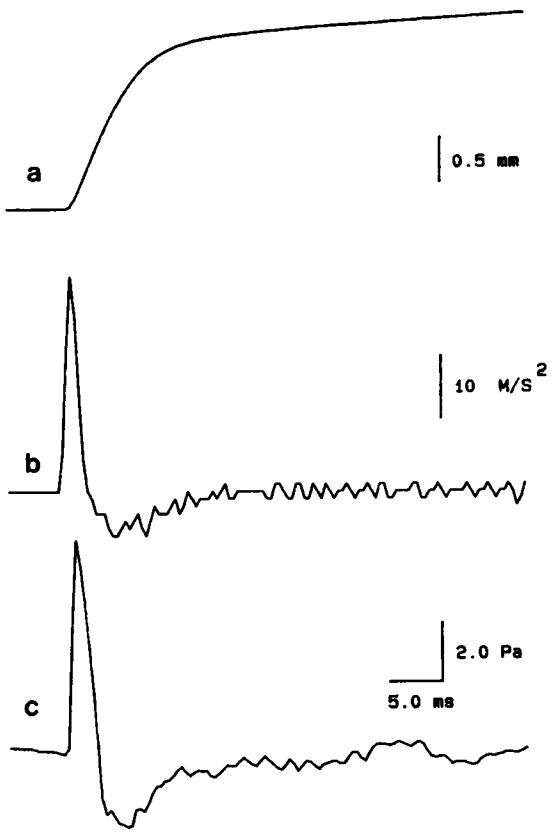

FIGURE 4 (*a*) The position of the end of the muscle nearest the hydrophone recorded by the servomotor as a function of time during a concentric contraction. Temperature for all three records (*a*, *b*, *c*) was 19.5°C. (*b*) The second derivative over time of the curve in Fig. 4 *a* corresponds to the linear acceleration of the muscle. The acceleration was calculated digitally and shown here as a function of time. (*c*) The acoustic signal was recorded simultaneously with the position signal during a concentric contraction. The hydrophone was positioned close to the long axis of the muscle. See the appendix for specific calculations of the relationship between acceleration and pressure amplitudes.

the product of muscle mass and linear acceleration. Subtracting the force record in Fig. 3 *b* from the force record in Fig. 3 *a* yields a function proportional to the linear acceleration of the muscle. Using a muscle mass of 0.3 g and a peak force of 0.026 N, the peak acceleration was 8.7 m/s^2. The pressure signal (Fig. 3 *c*) had essentially the same waveform as the linear acceleration and had a peak value of ~1.3 Pa. Eq. 3 *b* predicts a peak pressure of 1.4 Pa (see Appendix). Measuring the muscle position with a servomotor allows the linear acceleration to be calculated directly, independent of muscle mass. Fig. 4 *a* shows the position signal recorded during a concentric contraction with the servomotor attached to the moving end of the muscle. The second derivative over time (Fig. 4 *b*) is the linear acceleration of the muscle. The pressure signal (Fig. 4 *c*) had essentially the same waveform as the linear acceleration. The peak acceleration in this case was ~34 m/s^2—plugging 34 m/s^2 into Eq. 3 *b* yields a predicted peak pressure of 5.6 Pa (see Appendix) which is of the same order of magnitude as the experimental value of 7.3 Pa (Fig. 4 *c*). The differences between predicted and actual pressures are probably related to the nonspherical muscle geometry and the changing distance between the muscle and the hydrophone during the concentric contractions. Despite these rough approximations, the predicted pressures are well within an order of magnitude of the experimental results.

To check the model field equations we mapped the acoustic field produced by muscle twitches. The pressure amplitude initially decayed as an inverse function of radial distance from the muscle. At a distance of approximately one muscle length, the amplitude started to decay at a rate corresponding to the square of the distance from the

muscle (Fig. 5 *a*). These findings are consistent with the cylindrical shape of the muscle. Also, pressure amplitude had a cosinusoidal dependence on azimuth (Fig. 5 *b*). We have not mapped the pressure field above or below the major plane of movement.

DISCUSSION

Pressure waves are generated by lateral movements during isometric muscle contractions and the pressure waveform is directly related to the lateral acceleration of the muscle. The pressure field is dominated by the near-field component of a dipole model. This near-field component is not a propagated sound wave so, under these conditions, the term "muscle sound" is inappropriate. Sourds may be generated when the pressure waves encounter a boundary such as a skin-air interface but the underwater pressure waves described here correspond more to hydrodynamic sloshing than to sound.

Isolated muscles in a tank radiate as a dipole but this may not be true for muscles in vivo. Frangioni et al. (1987) report that the pressure waves from muscles in intact frog legs are, in fact, qualitatively the same as from muscles in vitro. However, stimulated human muscles produce pressure waves (Bolton et al., 1986) that have lower frequency components than frog muscle. The human muscles studied include small muscles such as the first dorsal interosseous

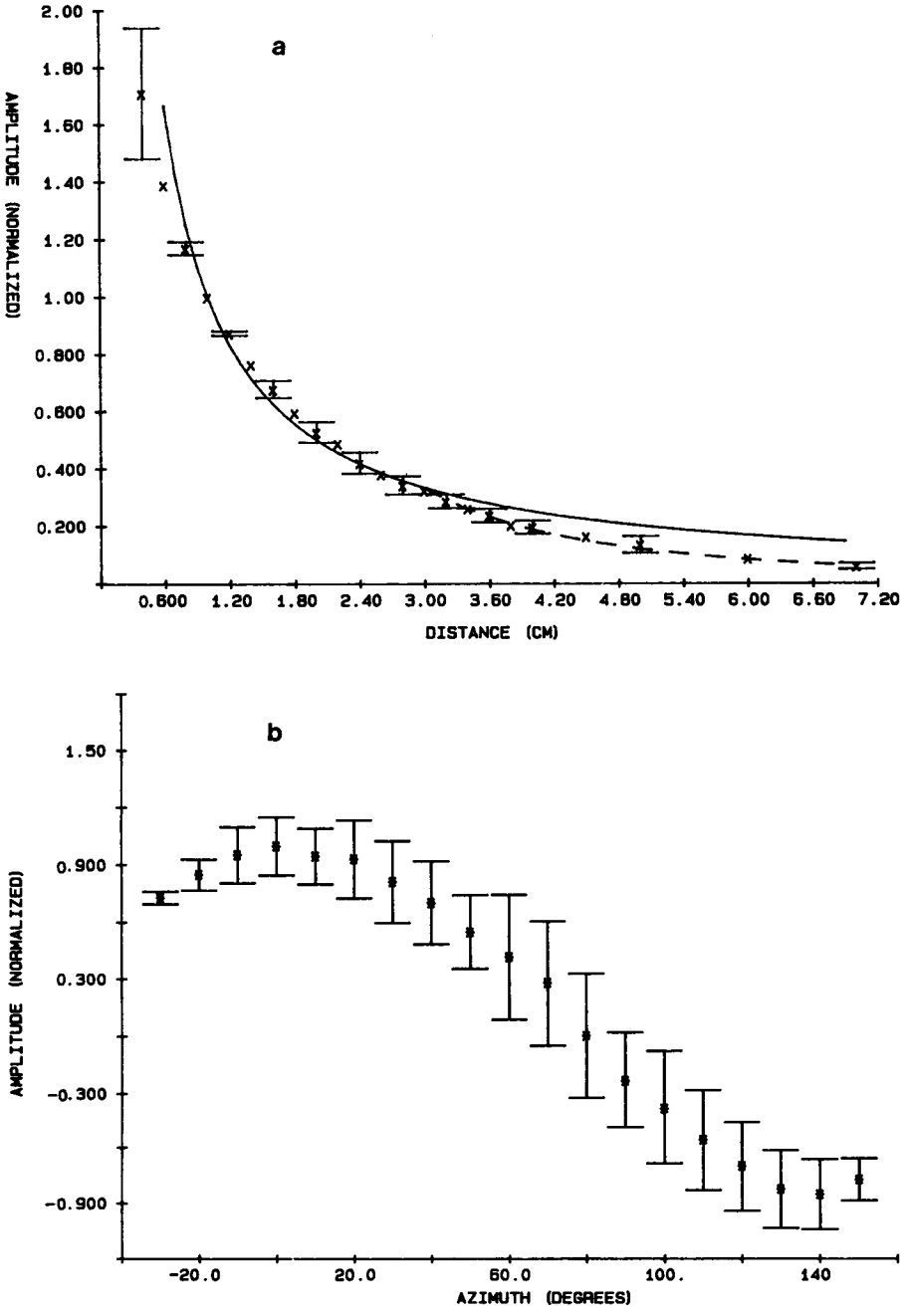

FIGURE 5 (*a*) The pressure amplitude is initially inversely proportional to distance from the muscle and then becomes proportional to the inverse square of the distance. Data are from five experiments, error bars are shown for every other point and denote standard deviation. The solid line is a $1/r$ function, and the dashed line is a $1/r\ r$ function, beginning at 3 cm. (*b*) The peak-to-peak pressure amplitude has a consinusoidal dependence on azimuth. Data are from four experiments.

muscle in the hand as well as larger muscles so that a larger mass is not the only reason for the presence of lower frequencies. Possibly the presence of adjacent muscles causes the human muscles to radiate with a plane wave source pattern rather than as a dipole. Further work is necessary to define the effects of adjacent musculature, muscle mass, and muscle topologies on the pressure signals.

The integrated signals seen here are interesting in that a large lateral movement is accompanied by smaller, superimposed oscillations. The large, slow muscle movement may be simply due to asymmetrical distribution of muscle fibers and nonsimultaneous contraction of fibers. If one side of the muscle pulls harder or earlier then lateral motion will occur. Since the acoustic signal is proportional to acceleration, the higher frequency oscillations dominate the signal recorded. These superimposed, smaller, higher frequency oscillations are interesting in that they appear to represent the natural mechanical response of the muscle to a step function input. The small oscillations occur at the resonant frequency of the muscle (Barry and Cole, 1988). The resonant frequency is related to stiffness, mass, length, and viscosity of the muscle and the surrounding medium. During an isometric twitch, however, the change in muscle stiffness is much greater than the change in any of the other parameters and may dominate the change in resonant frequency. If so, the sound signal can be used as a monitor of muscle stiffness changes during a twitch and therefore could provide information regarding crossbridge dynamics during a twitch.

APPENDIX

Eqs 3 a, b, and c can be used to roughly approximate the actual pressure recorded from a particular muscle. Using the following parameters, we compared the experimental results in Fig. 2 with the highly idealized model of a vibrating sphere described by the equations:

$w = 260$ rad/s
$u_o = 0.02$ m/s
$\rho_o = 1{,}026$ kg/(meter)^3
(seawater density (Kinsler, 1982)
$a_o = 0.006$ m
$S_o = 4.0 \times 10^{-4}$ m^2
$r = 0.012$ m
$c = 1{,}500$ m/s
(seawater sound velocity (Kinsler, 1982)
$k = 0.17$ m^{-1}
$\theta = 0°$

These parameters were obtained from the marked section of Fig. 2 *b* since this part of the waveform approximated one cycle of a harmonic vibration. The period of the cycle is 24 ms corresponding to a frequency of 42 Hz or 260 rad/s. Maximum velocity is obtained from the position points marked by arrows in Fig. 2 *b*; the distance between the points was 0.11 mm and the time between the points was 5.0 ms, yielding a velocity of 0.02 m/s. The actual muscle shape approximated a cylinder rather than a sphere, so the muscle surface area was calculated as the product of muscle length (3.0 cm) and circumference (1.3 cm), yielding a value of 4. $\times 10^{-4}$ m^2. The radius of a sphere with this area is 0.6 cm. The distance between the muscle and the hydrophone was 1.2 cm. Using these very rough approximations, Eq. 3 b predicts a pressure amplitude (half the peak-to-peak amplitude) of 3.5 Pa in phase with the muscle surface acceleration. Eq. 3 a predicts a pressure amplitude of 0.007 Pa that leads the surface acceleration by 90°. The term from Eq. 3 a is much smaller than the term from Eq. 3 b and the term from Eq. 3 b is of the same order of magnitude as the actual pressure of 3.8 Pa shown in Fig. 2 *a*.

A similar calculation can be made for the longitudinal accelerations shown in Figs. 3 and 4. In these cases, the hydrophone is positioned near the end of the muscle and longitudinal, rather than lateral, movement is monitored. The surface area "seen" by the hydrophone corresponds to the end of the muscle, so the actual muscle radius is used for the parameters of radius and surface area:

$a_o = 0.002$ m
$S_o = 5.0 \times 10^{-5}$ m^2
(surface of a sphere with radius 0.002)
$r = 0.005$ m

Fig. 4 shows a peak acceleration (wu_o) 0f 34 m/s^2. Plugging these parameters into Eq. 3 b yields a predicted peak pressure of 5.6 Pa which is of the same order of magnitude as the experimental value of 7.3 Pa. Fig. 3 shows a peak force of 0.026 N which corresponds to an acceleration of 8.7 m/s^2 for a mass of 0.003 Kg. Using the same parameters as for the data in Fig. 4, the predicted peak pressure is 1.4 Pa. The experimental peak pressure (Fig. 3 *c*) value is 1.3 Pa.

We thank T. McMahon for helpful discussions.

This work was supported by grant #NS-01017 from the National Institutes of Health, and the Grass Foundation.

Received for publication 6 July 1987 and in final form 18 December 1987.

REFERENCES

Barry, D. T., and N. M. Cole. 1988. Muscle sounds occur at the resonant frequency of skeletal muscle. Biophys. J. 53:571. (Abstr.)

Barry, D. T. 1987. Acoustic signals from frog skeletal muscle *Biophys. J.* 51:769–773.

Barry, D. T., S. R. Geringer, and R. D. Ball. 1985. Acoustic myography: a non-invasive monitor of motor unit fatigue. *Muscle Nerve.* 8:189–194.

Bolton, C. F., T. Parkes, and R. T. Thompson. 1986. Recordings of Electricity, Sound, and Force Arising from Human Muscle. *Muscle and Nerve.* 9:652.

Frangioni, J. V., T. S. Kwan-Gett, L. E. Dobrunz, and T. A. McMahon.

1987. The mechanism of low-frequency sound production in muscle. *Biophys. J.* 51:775–783.

Julian, F. J., and D. L. Morgan. 1979. Intersarcomere dynamics during fixed-end tetanic contractions of frog muscle fibers *J. Physiol. (Lond.).* 293:365–378.

Kinsler, L. E., A. R. Frey, A. B. Coppens, and J. V. Sanders. 1982. Fundamentals of fluid mechanics. John Wiley and Sons, Inc., New York.

Oster, G., and J. S. Jaffe. 1980. Low frequency sounds from sustained contraction of human skeletal muscle. *Biophys. J.* 30:119–127.

Ross, D. 1987. Mechanics of Underwater Noise. Peninsula Publishing, Los Altos, NY.

Ziomek, L. J. 1985. Underwater Acoustics: A linear systems theory approach. Academic Press, Inc. London.